Plant Biotechnology Journal
Open Access

Plant Biotechnology Journal (2020) **18**, pp. 141–154 doi: 10.1111/pbi.13182

Overexpression of *FBR41* enhances resistance to sphinganine analog mycotoxin-induced cell death and *Alternaria* stem canker in tomato

Zhiyong Shao[1,†], Yanting Zhao[2,†], Lihong Liu[1], Shanshan Chen[1], Chuanyou Li[3], Fanliang Meng[1], Haoran Liu[1], Songshen Hu[1], Jiansheng Wang[2,*] and Qiaomei Wang[1]

[1]*State Agricultural Ministry Laboratory of Horticultural Crop Growth and Development, Department of Horticulture, Zhejiang University, Hangzhou, China*
[2]*Institute of Vegetables, Zhejiang Academy of Agricultural Sciences, Hangzhou, China*
[3]*State Key Laboratory of Plant Genomics, National Centre for Plant Gene Research (Beijing), Institute of Genetics and Developmental Biology, Chinese Academy of Sciences, Beijing, China*

Received 25 July 2018;
revised 2 May 2019;
accepted 29 May 2019.
**Correspondence* (Tel +86 571 86094773; fax +86 571 86094773; email wangjs@mail.zaas.ac.cn or Tel 86-571-85909333; fax 86-571-88766022; email qmwang@zju.edu.cn)
[†]Both authors contributed equally to this work.

Keywords: *Alternaria alternata* f. sp. *lycopersici*, AAL-toxin, *Fumonisin B1 Resistant41*, programmed cell death, sphinganine analog mycotoxin, tomato.

Summary

Fumonisin B1 (FB1) and *Alternaria alternate* f. sp. *lycopersici* (AAL)-toxin are classified as sphinganine analog mycotoxins (SAMTs), which induce programmed cell death (PCD) in plants and pose health threat to humans who consume the contaminated crop products. Herein, *Fumonisin B1 Resistant41* (*FBR41*), a dominant mutant allele, was identified by map-based cloning of *Arabidopsis* FB1-resistant mutant *fbr41*, then ectopically expressed in AAL-toxin sensitive tomato (*Solanum lycopersicum*) cultivar. *FBR41*-overexpressing tomato plants exhibited less severe cell death phenotype upon AAL-toxin treatment. Analysis of free sphingoid bases showed that both *fbr41* and *FBR41*-overexpressing tomato plants accumulated less sphinganine and phytosphingosine upon FB1 and AAL-toxin treatment, respectively. *Alternaria* stem canker is a disease caused by AAL and responsible for severe economic losses in tomato production, and *FBR41*-overexpressing tomato plants exhibited enhanced resistance to AAL with decreased fungal biomass and less cell death, which was accompanied by attenuated accumulation of free sphingoid bases and jasmonate (JA). Taken together, our results indicate that *FBR41* is potential in inhibiting SAMT-induced PCD and controlling *Alternaria* stem canker in tomato.

Introduction

Programmed cell death (PCD) is an active suicide process that leads to selective removal of unwanted or severely damaged cells, which occurs during development, senescence, as well as response to abiotic and biotic stress (Das *et al*., 2010). Necrotrophic pathogens that obtain nutrients from the dead cells have developed a strategy to successfully elicit PCD of their hosts by secreting mycotoxins (Walton, 1996). Fumonisin B1 (FB1) and *Alternaria alternate* f. sp. *lycopersici* (AAL)-toxin are two well-studied mycotoxins, produced by *Fusarium* species and *Alternaria alternate*, respectively (Abbas *et al*., 1994). They are classified as sphinganine analog mycotoxins (SAMTs) because of their structural similarity to sphinganine, the backbone precursor of sphingolipids.

The underlying mechanism of SAMT-induced PCD is associated with the competitive inhibition of ceramide synthase, which suppresses the conversion of sphinganine, phytosphingosine and other free sphingoid bases to complex ceramides. The resultant accumulation of free sphingoid bases acts as a second message to activate transduction pathways of PCD elicitation (Lachaud *et al*., 2013; Saucedo-Garcia *et al*., 2011; Shi *et al*., 2007). *De novo* biosynthesis of free sphingoid bases is initiated by serine palmitoyltransferase (SPT), which catalyses the condensation of serine and palmitoyl-CoA to form intermediate 3-ketosphingosine. The product of this reaction is then reduced to sphinganine, the simplest free sphingoid base (Chen *et al*., 2010; Lynch and Dunn, 2004). Further modification of sphinganine is conducted by the addition of a hydroxyl group at C4 to yield phytosphingosine and/or by introduction of double bonds at C4 and C8 to produce other free sphingoid bases (Chen *et al*., 2010; Lynch and Dunn, 2004). Different from a soluble homodimer in some bacterial, SPT is an endoplasmic reticulum (ER)-localized heterodimer comprised of long chain base 1 (LCB1) and LCB2 subunits in all known eukaryotes (Chen *et al*., 2006; Dietrich *et al*., 2008; Ikushiro *et al*., 2001; Tamura *et al*., 2001). The catalytic lysine residue that binds with pyridoxal 5′ phosphate is located in LCB2 subunit and LCB1 is able to stabilize LCB2 (Hanada, 2003; Tamura *et al*., 2001). In addition, another smaller subunit, termed the small subunit of SPT (ssSPT), also interacts with the LCB1/LCB2 subunits. The ssSPTs usually enhance SPT activity by stabilizing SPT complex, which has been shown in *Arabidopsis* with *ssSPT* overexpression leading to increased SPT activity and *ssSPT* suppression resulting in reduced SPT activity (Kimberlin *et al*., 2013). There is one *AtLCB1* (*At4g36480*) gene and two homologous *LCB2* genes, *AtLCB2a* (*At5g23680*) and *AtLCB2b* (*At3g48780*) in *Arabidopsis*. The expression of *AtLCB2a* is usually higher than that of *AtLCB2b* (Dietrich *et al*., 2008). Partial suppression of *AtLCB1* led to enhanced resistance to FB1, which was accompanied by decreased accumulation of free sphingoid bases (Shi *et al*., 2007). A null mutant of *AtLCB2a* also displayed FB1-resistant phenotype and attenuated accumulation of free sphingoid bases (Saucedo-Garcia *et al*., 2011). These results link the function of SPT as a PCD regulator to free sphingoid bases.

AAL is the causal agent of *Alternaria* stem canker in tomato in several parts of the world (Grogan *et al*.,1975; Kohmoto *et al*., 1982; Malathrakis, 1983), leading to serious economic losses in tomato production. The disease symptom occurs in the form of dark-brown concentric cankers on stems and necrosis spots on leaves (Grogan *et al*., 1975). AAL pathogenicity depends on the

production of AAL-toxin, as toxin-deficient AAL mutants neither colonize nor cause symptoms in susceptible tomato cultivars (Akamatsu *et al*., 1997). Resistance to AAL and AAL-toxin has been reported to be controlled by the single co-dominant *Alternaria stem canker* (*Asc*) locus (Brandwagt *et al*., 2000; Mesbah *et al*., 1999). The *Asc-1* gene isolated from resistant tomato genotype could salvage the transportation of glycosilphosphatidylinositol anchored proteins from ER to Golgi through production of alternative ceramides (Brandwagt *et al*., 2000). Quantitative analysis of free sphingoid bases demonstrated that the tomato with resistant *Asc/Asc* genotype accumulated about half the levels of sphinganine and phytosphingosine than the one with susceptible *asc/asc* genotype when treated with AAL-toxin (Abbas *et al*., 1994), suggesting that *Asc* could prevent the build-up of free sphingoid bases induced by AAL-toxin, thus enhancing the resistance of tomato to AAL-toxin.

Phytohormone signalling pathways have a critical role in regulation of plant defence against pathogen attack, among which jasmonate (JA)-dependent pathway is usually effective against necrotrophic pathogens and salicylic acid (SA)-dependent responses counteract biotrophic pathogens (Glazebrook, 2005). However, in tomato–AAL interaction system, JA promotes the susceptibility of tomato to AAL. Disease development and *in planta* growth of AAL were decreased in JA-deficient mutants and increased in prosystemin-overexpressing transgenic lines (*35S::prosystemin*) which constitutively accumulate high level of JA. Exogenous application of methyl jasmonate (MeJA) restored disease symptom of JA-deficient mutants to wild-type (WT) level and led to increased disease symptom in WT (Egusa *et al*., 2009; Jia *et al*., 2013). In contrast to JA signalling pathway, SA-dependent pathway has been shown to enhance the resistance of tomato to AAL. Pretreatment of SA greatly decreased lesion occurrence after AAL infection, and transgenic plants defective in SA accumulation (*NahG*) exhibited more expanding lesions with higher amount of fungal than WT (Jia *et al*., 2013).

Although several molecular components and pathways involved in the resistance of plants to SAMT-induced PCD and SAMT-producing pathogens have been identified in model plants, their application in crop production is limited, and the related molecular mechanisms remain to be further elucidated. Herein, we have identified a dominant mutant allele, *Fumonisin B1 Resistant41* (*FBR41*) by map-based cloning of FB1-resistant mutant in *Arabidopsis*. Ectopic overexpression of *FBR41* conferred an increased insensitivity to AAL-toxin and mediated resistance to *Alternaria* stem canker in tomato. The results provide a potential strategy for controlling SAMT contamination and diseases caused by SAMT-producing pathogens in crops.

Results

Identification, phenotypic and genetic analysis of *fbr41* mutant

Approximately 15 000 ethyl methanesulfonate (EMS)-mutagenized *Arabidopsis* M2 seeds were germinated on half-strength MS medium containing 1 μM FB1, and a FB1-resistant mutant, designated as *fumonisin b1 resistant 41* (*fbr41*), was isolated (Figure 1a). Then, the mutant was self-fertilized, and the resulting progeny (M3) were all resistant to FB1.

To further analyse the sensitivity of *fbr41* to FB1, the mutant and WT (Col-0) were grown on half-strength MS medium containing 1.5 μM FB1 or infiltrated with 10 μM FB1 solution on leaves. FB1 seriously inhibited the growth of WT but hardly affected the growth of *fbr41* (Figure 1c). When rosette leaves of six-week-old plants were infiltrated with 10 μM FB1 solution, the FB1-treated leaves of WT exhibited hypersensitive response-like lesions at 3 days postinfiltration. In contrast, no obvious lesions were observed on the leaves of *fbr41* plant (Figure 1d). Of note, *fbr41* displayed dwarf phenotype in the absence of FB1 (Figure 1b,d), while had no defects in reproductive growth.

When *fbr41* was backcrossed with parent Col-0, F_1 progeny were resistant to FB1 (Figure 1e), and F_2 population derived from self-fertilized F_1 plants segregated in a 3:1 ratio (FB1-resistant: sensitive = 535:182, $\chi^2 = 0.637$, $P = 0.73$). These results suggest that the FB1-resistant phenotype of *fbr41* is controlled by a single dominant Mendelian locus.

Map-based cloning of *FBR41*

A map-based cloning strategy was used to isolate the *FBR41* locus in a population generated from a cross between *fbr41* and *Arabidopsis* ecotype *Landsberg erecta*.

A total of 23 pairs of simple sequence length polymorphism (SSLP) markers (Table S2) were selected for first-pass mapping of *FBR41*, and *FBR41* was first mapped to the bottom arm of chromosome 3 in the interval between molecular markers T24C20 and T18N14 (Figure 2a). Subsequent fine mapping of the gene was performed in a total of 2500 FB1-resistant individuals with cleaved amplified polymorphic sequences (CAPS) markers (Table S3), and *FBR41* was delimited to an interval flanked by molecular markers 18005CAPS and 18175CAPS.

Within the identified region, the causative mutation was predicted according to the annotation and function displayed in Cereon tair database (http://arabidopsis.org/). Among these genes, we identified a gene encoding AtLCB2b subunit of SPT (*At3g48780*), which catalyses the first step of sphingolipid biosynthesis and is involved in SAMT-induced PCD based on previous studies (Saucedo-Garcia *et al*., 2011; Shi *et al*., 2007; Spassieva *et al*., 2002). Therefore, we examined genomic DNA sequence of *At3g48780* in *fbr41*. A nucleotide substitution from G to A was identified at the splicing junction of the first exon and the first intron in *At3g48780* (Figure 2b), which was predicted to cause splicing error of *At3g48780* pre-mRNA. To check the transcription of *At3g48780* in *fbr41* mutant, we amplified and sequenced the full-length *At3g48780* complementary DNA (cDNA) in *fbr41*. A five base-pair (ATTTT) insertion between the first and second exon was observed in the *At3g48780* transcript in *fbr41* (Figure 2b), which was predicted to introduce a premature stop codon and produce a putative protein with the first 42 amino acids of the annotated 489 amino acids of WT protein plus 52 additional amino acids before a premature stop codon (Figure S2). Furthermore, we conducted quantitative RT-PCR to examine if the expression level of *At3g48780* was altered *in fbr41*. As shown in Figure 2d, there was no difference between WT and *fbr41* in the abundance of *At3g48780* transcripts (Figure 2d).

FB1-resistant phenotype is controlled by a dominant locus, to confirm that the G-to-A transition in *At3g48780* is responsible for the dominant phenotype, transgenic plants expressing the mutant *At3g48780* allele under CaMV 35S promoter (35S::*FBR41*) was generated in the WT background, and their phenotypes were observed. As expected, transgenic lines presented similar FB1-resistant phenotypes with *fbr41*, with fewer lesions than WT after FB1 infiltration (Figure 2e). Accordingly, the extent of tissue damage as indicated by relative conductivity in transgenic plants leaves upon FB1 infiltration was significantly lower

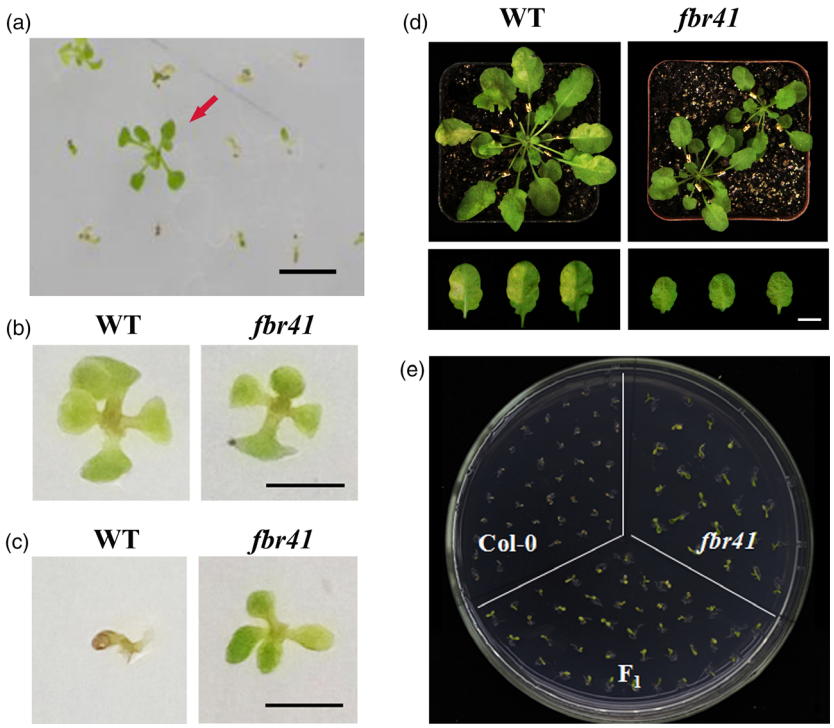

Figure 1 Isolation, phenotypic and genotypic characterization of fumonisin B1 (FB1)-resistant mutant *fbr41*. (a) Isolation of FB1-resistant mutant *fbr41*. An ethyl methanesulfonate (EMS)-generated mutant population seeds were sown on half-strength MS medium containing 1.5 μM FB1, and FB1-resistant individual (indicated by red arrow) was isolated for further identification. (b,c) Phenotypes of wild-type (Col-0) and *fbr41* seedlings grown on half-strength MS medium containing 0.15% methanol (v/v) (b) or 1.5 μM FB1 (c), photographs were taken 14 days after sowing. (d) Typical phenotypes of FB1-induced programmed cell death. Six-week-old WT and *fbr41* were infiltrated with 10 μM FB1 (left half of treated leaves) and 1% (v/v) methanol as control (right half of treated leaves), then photographed at 3 days postinjection (DPI). (e) FB1 resistance of F_1 progeny derived from crosses between *fbr41* and Col-0 plants. Scale bars = 1 cm (a–d).

than that of WT (Figure 2f). Therefore, it is convincible that the FB1-resistant phenotype of *fbr41* is the result of a single nucleotide mutation in *At3g48780*.

FBR41 attenuates the increase in free sphingoid bases upon FB1 treatment

As *FBR41* corresponds to *AtLCB2b*, which encodes an essential subunit of SPT, we supposed that the FB1-resistant phenotype of *fbr41* and *FBR41*-overexpressing lines is potentially related to altered accumulation of free sphingoid bases, the putative downstream products of SPT (Figure 3a). To confirm the assumption, we compared the accumulation of specific free sphingoid bases in *fbr41, FBR41*-overexpressing lines and WT with or without FB1 treatment. Total free sphingoid bases were selectively extracted from leaves of 6-week-old plants and quantitatively analysed by LC-MS/MS. Individual free sphingoid base was identified by the retention of corresponding standard. Free sphingoid bases analysed included sphinganine and phytosphingosine, which were abundant and most affected by FB1 according to previous studies (Saucedo-Garcia *et al*., 2011; Shi *et al*., 2007). The results showed that the levels of free sphingoid bases in *fbr41* or transgenic lines under control condition were low and showed no significant difference compared to WT (Figure 3b), suggesting that the mutation did not affect basal levels of free sphingoid bases. Dramatic increase in free sphingoid bases was observed at 6 h after FB1 exposure, in agreement with the previous reports (Saucedo-Garcia *et al*., 2011; Shi *et al*., 2007). However, the contents of sphinganine and phytosphingosine in *fbr41* were 30% and 74% of those in WT, respectively (Figure 3b). FB1-treated *FBR41*-overexpressing lines also produced low levels of sphinganine and phytosphingosine, similar to those exhibited by *fbr41* (Figure 3b). The findings demonstrate that increased resistance to FB1 in *fbr41* as well as *FBR41*-overexpressing lines is associated with attenuated accumulation of free sphingoid bases.

FBR41 impacts the *in vivo* interaction between AtLCB1 and AtLCB2a

In *Arabidopsis*, AtLCB1 interacts with AtLCB2 to form a functional SPT (Chen *et al*., 2006; Dietrich *et al*., 2008; Shi *et al*., 2007). *FBR41* is a mutant allele of *AtLCB2b*, encoding an abnormal protein with 94 amino acids (Figure S2). To test whether FBR41 interacts with AtLCB1, luciferase complementation imaging (LCI) assay was conducted, in which FBR41 and AtLCB1 were fused to the C-terminal fragment (FBR41-Cluc) and N-terminal fragment (AtLCB1-Nluc) of the firefly luciferase (LUC) enzyme. Co-expression of FBR41-Cluc with AtLCB1-Nluc resulted in strong luminescence signal in the leaves of *N. benthamiana*, whereas co-expression of AtLCB1-Nluc/Cluc, FBR41-Cluc/Nluc and an unfused Nluc/Cluc pair, as three negative controls, showed only background levels of luminescence (Figure 4a,b). Western blot confirmed the similar expression levels of Nluc- and Cluc-fusion proteins in different treatments (Figure 4c), suggesting that the strong luminescence output detected from co-expressed AtLCB1-Nluc/FBR41-Cluc was not resulted from high levels of AtLCB1-Nluc and FBR41-Cluc proteins, but rather dominated by the specific interaction between AtLCB1 and FBR41. The results demonstrate that FBR41 could interact with AtLCB1 *in vivo*.

The *in vivo* interaction between FBR41 and AtLCB1 promoted us to speculate that FBR41 might impact the interaction between AtLCB1 and AtLCB2. To verify the assumption, we transiently expressed FBR41 with AtLCB1-Cluc/AtLCB2a-Nluc pair in *N. benthamiana* leaves and examined whether the introduction of FBR41 could impact the *in vivo* interaction between AtLCB1 and AtLCB2a. As shown in Figure 4d, a strong luminescence signal was obtained when co-expressing AtLCB2a-Nluc/AtLCB1-Cluc plus empty vector (control), indicating the *in vivo* interaction between AtLCB1 and AtLCB2a. However, co-expression of AtLCB2a-Nluc/AtLCB1-Cluc plus FBR41 produced substantially reduced luminescence output,

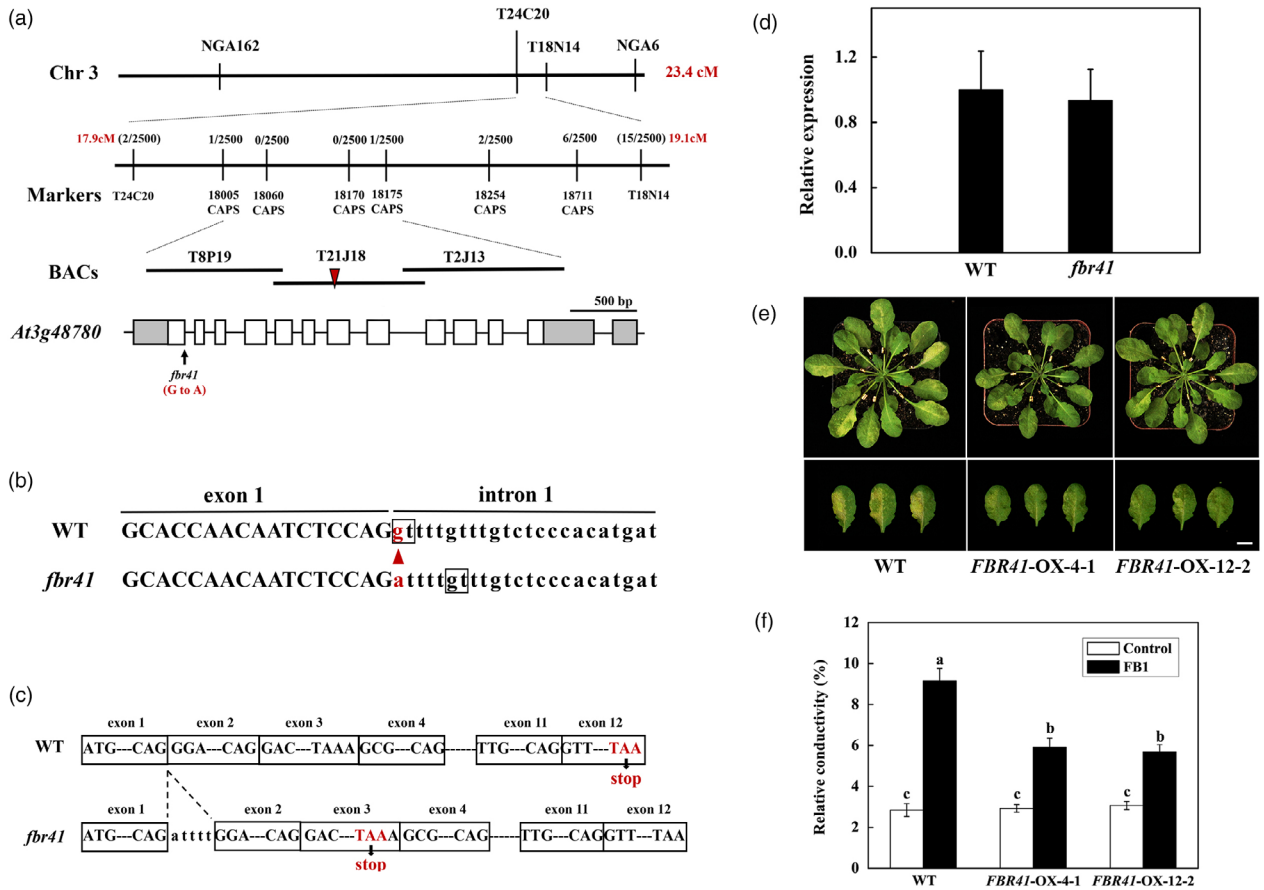

Figure 2 Map-based cloning of *FBR41*. (a) Map-based cloning of *FBR41* locus. An arrowhead indicates a G-to-A substitution in *At3g48780* locus in *fbr41*. Grey boxes and white boxes indicate UTR and exons, respectively, and line segments represent introns. BACs, bacterial artificial chromosomes. (b) Genomic DNA sequence of *At3g48780* in wild type (WT) and *fbr41*. The triangle shows the mutation in the splicing junction of the exon 1 and the intron 1 in *At3g48780*. The nucleotides in boxes indicate the 5′ splice donor sites. (c) A five base-pair insertion (ATTTT) between exon 1 and exon 2, and a premature stop codon at exon 3 in the *At3g48780* transcripts in *fbr41*. (d) Quantitative RT-PCR analysis of the *At3g48780* transcripts in WT and *fbr41*. (e) Phenotypes of *FBR41*-overexpressing plants upon FB1 treatment. Photographs were taken at 3 days postinjection (DPI). Scale bar = 1 cm. (f) Quantitative measurements of relative conductivity in treated leaves at 3 DPI. Six representative leaves from three plants were collected and pooled as one sample. Data shown are means ± SD of three biological replicates. Different letters denote a statistically significant difference from control-infiltrated WT (one-way ANOVA, $P < 0.05$, Tukey's test).

compared with that of control (Figure 4d,e). Western blot showed that the expression levels of the AtLCB2a-Nluc and AtLCB1-Cluc were similar between AtLCB2a-Nluc/AtLCB1-Cluc/empty vector and AtLCB2a-Nluc/AtLCB1-Cluc/FBR41-myc groups (Figure 4f), suggesting that FBR41 did not impact the expression of AtLCB1 and AtLCB2a, but rather disrupted the *in vivo* interaction between AtLCB1 and AtLCB2a.

Generation of *FBR41*-overexpressing tomato plants

Based on the results that *FBR41* mediates resistance to FB1 in *Arabidopsis*, we further explored the role of *FBR41* in SAMT resistance in phylogenetically distant tomato plants. A construct containing *FBR41* driven by cauliflower mosaic virus (CaMV) 35S promoter was introduced into AAL-toxin sensitive tomato cultivar. Nine independent transgenic lines were obtained (Figure 5a), and five lines were confirmed to carry single transgenic insertion based on segregation analysis on T_1 seeds (kanamycin resistance: kanamycin sensitive = 3:1). Homozygous *FBR41* lines were selected from self-pollinated *FBR41*-overexpressing plants of T_1 generation and verified by semi-quantitative RT-PCR (Figure 5b).

We randomly chose two homozygous *FBR41*-overexpressing lines for analysis of phenotypes. Plant height, morphology and leaf size of *FBR41*-overexpressing plants were indistinguishable from WT (Figure 5c). Furthermore, no significant differences between transgenic plants and WT were observed for flowering time, fruit development and yield (Table 1; Figure 5d,e). These results show that *FBR41* have no negative pleiotropic effects on plant growth and development.

Ectopic expression of *FBR41* enhances resistance to AAL-toxin-induced cell death in tomato

To investigate the effect of *FBR41* on resistance to AAL-toxin-induced cell death in tomato, detached leaflets of *FBR41*-overexpressing plants and WT were treated with 0.2 μM AAL-toxin, and PCD symptom was observed continuously. Visible black necrotic lesions, the typical AAL-toxin-induced symptom as previously reported (Mesbah *et al.*, 2000; Zhang *et al.*, 2011), were observed on the leaflets of sensitive tomato cultivars at 48 h after toxin treatment (Figure 6a). However, toxin-treated leaflets of *FBR41*-overexpressing plants displayed minor necrotic lesions and lower relative conductivity compared to WT (Figure 6a,b). As

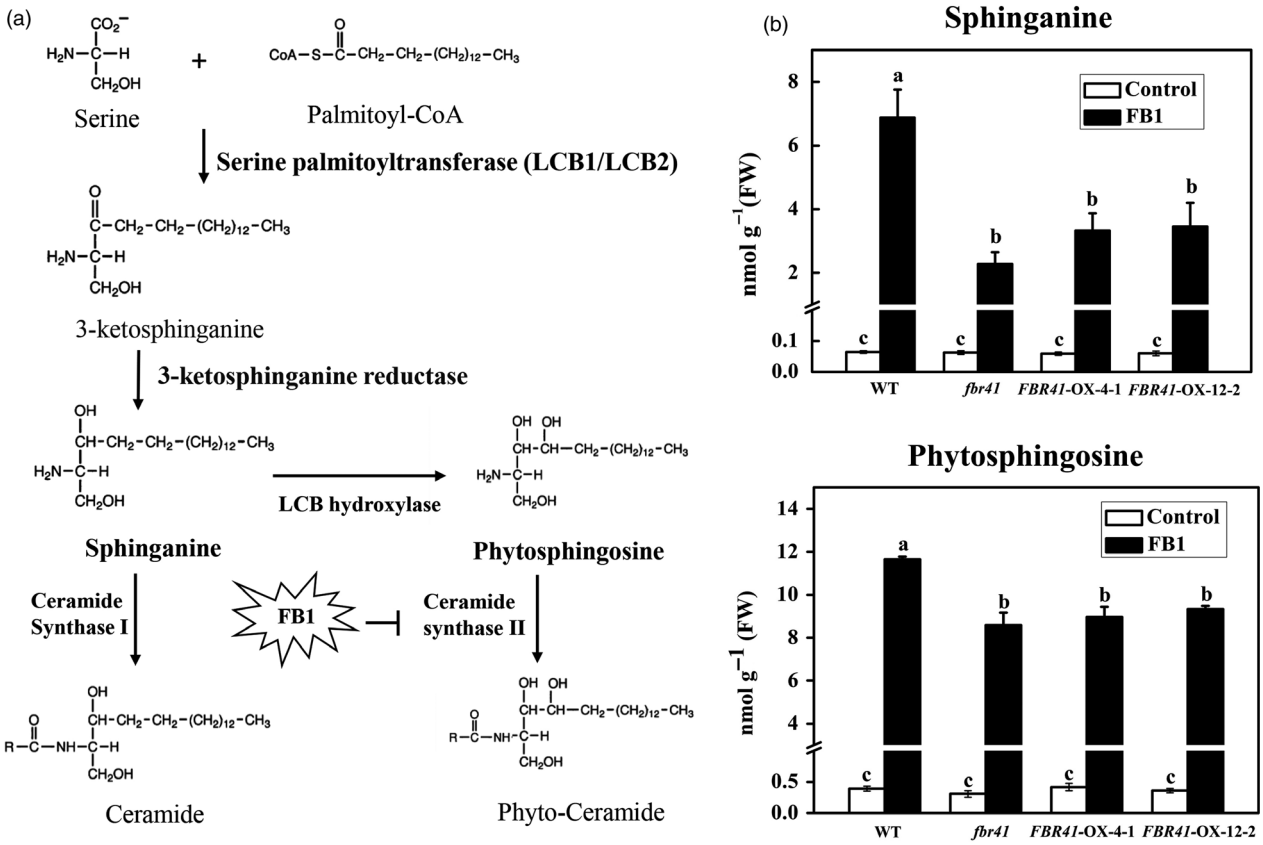

Figure 3 Biosynthetic pathway of free sphingoid bases and their contents in wild-type (WT), *fbr41* and *FBR41*-overexpressing plants. (a) Biosynthesis of free sphingoid bases. *De novo* synthesis of free sphingoid bases is initiated through condensation of serine and palmitoyl-CoA, which is catalysed by serine palmitoyltransferase (SPT). The product of SPT is immediately reduced to the simplest free sphingoid base sphinganine, which is further modified by the addition of a hydroxyl group at C4 to yield phytosphingosine. Both sphinganine and phytosphingosine can be converted into ceramide and phyto-ceramide, respectively, by ceramide synthase. Fumonisin B1 (FB1) is the potential competitive inhibitor of ceramide synthase II, leading to accumulation of phytosphinsoine as well as sphinganine. (b) Contents of free sphingoid bases in WT, *fbr41* mutant and *FBR41*-overexpressing transgenic lines. Six-week-old plants were injected with 10 μM FB1 or 1% methanol (v/v, control), and samples were harvested at 6 h postinjection. Data shown are means ± SD of three biological replicates. Different letters denote a statistically significant difference among treatment (one-way ANOVA, $P < 0.05$, Tukey's test). FW, fresh weight.

different transgenic lines exhibited similar disease symptom (Figure 6a), we chose *FBR41*-OX-3 as a representative transgenic line for further analysis.

Considering *FBR41* alters the accumulation of free sphingoid bases upon FB1 treatment in *Arabidopsis*, we also analysed these compounds in leaflets of *FBR41*-overexpressing tomato plants. The levels of sphinganine and phytosphingosine were low with no obvious difference between *FBR41*-overexpressing plants and WT under control (Figure 6c). Marked increase in sphinganine and phytosphingosine was attained after AAL-toxin treatment in both *FBR41*-overexpressing plants and WT at 48 h of toxin treatment (Figure 6c). However, the levels of sphingosine and phytosphingosine in *FBR41*-overexpressing tomato leaflets were 64% and 79% of those in WT, respectively (Figure 6c). The results provide a link between enhanced resistance to AAL-toxin-induced PCD and attenuated accumulation of free sphingoid bases in *FBR41*-overexpressing tomato plants.

Ectopic expression of *FBR41* enhances resistance to *Alternaria* stem canker in tomato

AAL-toxin is a host-specific pathogenicity factor of necrotrophic pathogen AAL, which causes *Alternaria* stem canker and leaf necrosis on susceptible tomato cultivars. *FBR41*-overexpressing tomato plants were more resistant to AAL-toxin; we then further tested the resistance of them to *Alternaria* stem canker. Typical necrotic lesions began to develop on leaves at approximately 3 days postinoculation (DPI) of AAL. As the disease progressed, the necrotic lesions enlarged and the infected leaves wilted and eventually died. Fewer lesions were observed in *FBR41*-overexpressing tomato plants at 3 DPI, compared with WT plants (Figure 7a; Figure S5). To quantify the extent of tissue damage and fungal biomass of AAL-infected leaves, electrolyte leakage and amount of fungal DNA were measured, respectively. Significantly lower relative conductivity (Figure 7b) and less fungal DNA (Figure 7d) were found in leaves of *FBR41*-overexpressing plants at 3 DPI when compared with the corresponding WT, which is consistence with the phenotypic assay. Along with the infection, we also found that leaves gradually lost chlorophyll and became yellow, which was consistent with previous studies (Meena *et al.*, 2016). However, delayed degradation of total chlorophyll was observed in *FBR41*-overexpressing plants upon AAL infection, compared to WT plants (Figure 7c). In sum, *FBR41* enhances resistance to *Alternaria* stem canker caused by AAL in tomato.

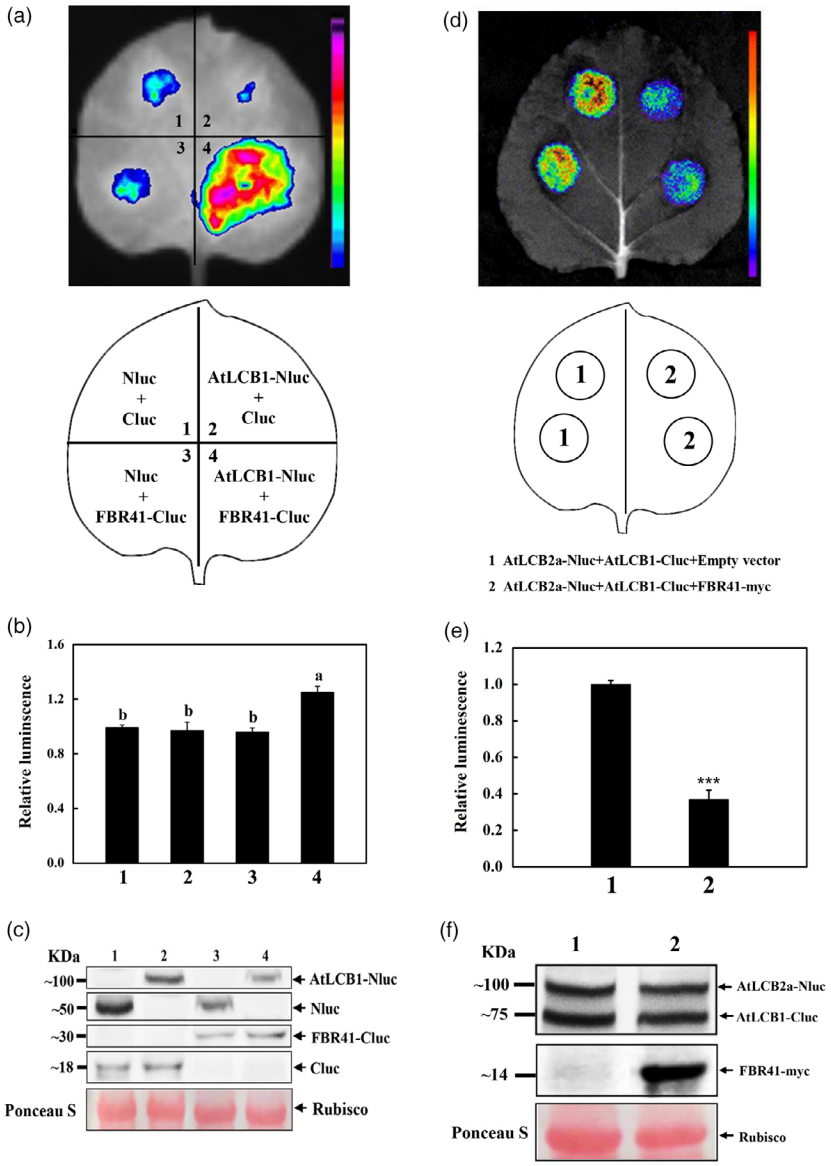

Figure 4 FBR41 disrupts the *in vivo* interaction between AtLCB1 and AtLCB2a (a) Luciferase complementation imaging (LCI) assays showing the interaction between FBR41 and AtLCB1. *Agrobacterium* harbouring AtLCB1-Nluc and FBR41-Cluc constructs were co-infiltrated into *N. benthamiana* leaves. Luminescence was monitored at 3 days postinfiltration. The Nluc/Cluc, AtLCB1/Cluc and Nluc/FBR41-Cluc pairs were used as negative control. (b) Quantitative analysis of luminescence intensity in different treatments as indicated in (a). Data are means ± SD of three biological replicates. Different letters denote a statistically significant difference from each other (one-way ANOVA, $P < 0.05$, Tukey's test). (c) Western blot showing the expression levels of Nluc- or Cluc-fusion proteins in agroinfiltrated leaf samples shown in (a). Ponceau S staining shows the equal loading of total proteins. (d) LCI assays showing that FBR41 disrupts the interaction between AtLCB1 and AtLCB2a. *Agrobacterium* carrying AtLCB1-Nluc/AtLCB2a-Cluc plus FBR41-myc were co-infiltrated into *N. benthamiana* leaves. Luminescence was monitored at 3 days postinfiltration. The AtLCB1-Nluc/AtLCB2a-Cluc/empty vector group was used as control. (e) Quantitative measurement of luminescence intensity in different treatments as indicated in (d). Data are means ± SD of three biological replicates. Asterisks denote statistically significant differences compared with control (Student's *t*-test, ***$P < 0.001$). (f) Western blot showing the expression levels of AtLCB2a-Nluc, AtLCB1-Cluc and FBR41-myc in agroinfiltrated leaf samples shown in (d). Ponceau S staining shows the equal loading of total proteins.

Further analysis of the free sphingoid bases showed that both sphinganine and phytosphingosine were significantly induced by AAL inoculation in *FBR41*-overexpressing tomato plants and WT (Figure 8a). There was no significant difference in free sphingoid bases between *FBR41*-overexpressing plants and WT without AAL inoculation (Figure 8a). However, the levels of sphinganine and phytosphingosine in *FBR41*-overexpressing tomato leaves at 3 DPI were 59% and 68% of those in WT, respectively (Figure 8a), which might account for the less foliar symptom in *FBR41*-overexpressing plants.

Phytohormones JA and SA are commonly known to modulate the susceptibility of tomato to AAL (Egusa *et al.*, 2009; Jia *et al.*, 2013); therefore, we also determined the levels of both phytohormones in *FBR41*-overexpressing tomato plants and WT. As shown in Figure 8b, there was no significant difference in endogenous SA content between *FBR41*-overexpressing plants

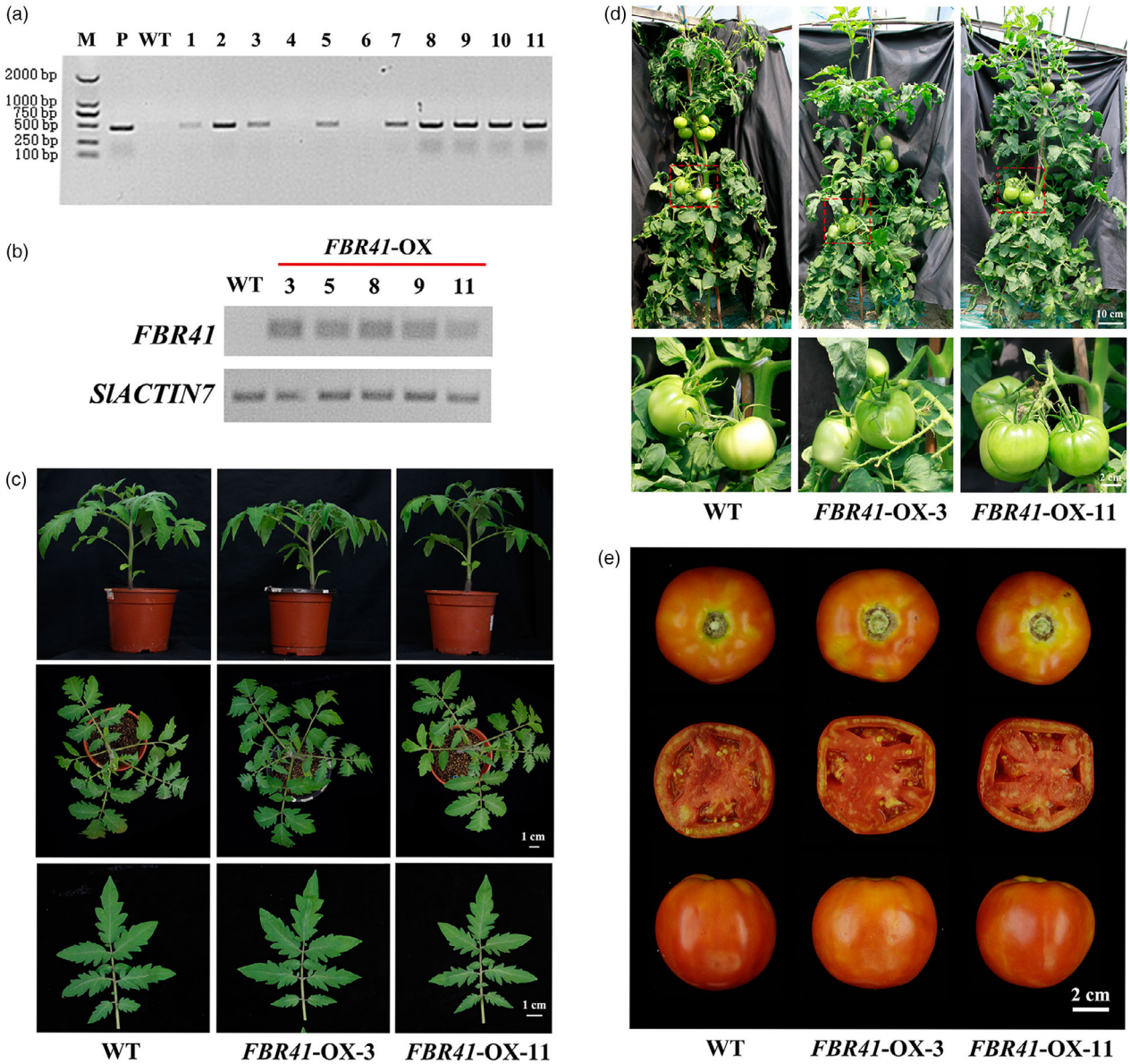

Figure 5 Genotyping and phenotyping analysis of *FBR41*-overexpressing tomato plants. (a) PCR analysis of putative T_0 transgenic plants using primers of *FBR41*-F and *MYC*-R. A 0.44-kb DNA fragment was amplified to identify positive transgenic plants. M: DL 2000 marker; P: positive control; WT: wild-type; Lane 1–11: putative T_0 transgenic lines. (b) Semi-quantitative RT-PCR analysis of homozygous transgenic plants containing single transgene insertions. (c–e) Effect of *FBR41* overexpression on plant height, morphology, leaf size (c), mature green fruits (d) and ripen fruits (e). In (c), the top and middle row shows 5-week-old tomato plants grown in phytotron and the bottom row shows 4th leaf of tomato plants. In (d), the top panel shows 4-month-old tomato plants grown in field and the dotted line represents the mature green (MG) tomato fruits. The bottom panel shows the magnified pictures of MG tomato fruits.

and WT with or without AAL treatment. Although the level of JA in *FBR41*-overexpressing plants was similar to that in WT under control treatment, *FBR41*-overexpressing plants accumulated less JA than WT after AAL inoculation. Considering AAL utilizes JA signalling pathway for successful invasion into the host as previously reported (Egusa *et al*., 2009; Jia *et al*., 2013), the inhibition of JA accumulation might account for less fungal biomass in *FBR41*-overexpressing plants.

Discussion

Based on the fact that micromolar levels of FB1 can efficiently inhibit growth of *Arabidopsis* seedlings, screening of FB1-resistant mutants has been used to identify genes involved in FB1-induced PCD. In this study, we have characterized *FBR41* through map-based cloning of FB1-resistant mutant in *Arabidopsis*, which carries a nucleotide substitution in the gene encoding AtLCB2b subunit of SPT. Different from previously reported mutant alleles by forward genetic approaches, all of which are recessive (Table S1), *FBR41* is the first dominant FB1-resistant mutant allele identified so far.

As the first step enzyme in sphingolipid biosynthesis, SPT plays a critical role in regulation of SAMT-induced PCD. Chemical treatment with myriocin, a potent SPT inhibitor, partially relieved the susceptibility of *Arabidopsis* to FB1, as well as tomato to AAL-toxin (Brandwagt *et al*., 2002; Shi *et al*., 2007). SPT functions as a

Table 1 Effect of *FBR41* on tomato flowering, fruit ripening and yield

Parameter	Wild type	*FBR41*-OX-3	*FBR41*-OX-11
Flowering time (days)	59.7 ± 1.6 a	60.5 ± 1.6 a	59.2 ± 1.2 a
Days from anthesis to fruit ripen	73.4 ± 1.8 a	74.6 ± 2.1 a	75.8 ± 1.7 a
Ripen fruits per plant	10.0 ± 1.1 a	10.3 ± 1.8 a	9.5 ± 1.3 a
Fruit weight (g)	133.33 ± 11 a	129.29 ± 9.1 a	131.43 ± 11.38 a
Fruit yield per plant (g)	1277.7 ± 42.9 a	1290 ± 45.4 a	1238 ± 41.1 a

Data shown are means ± SD for 16 plants grown in glasshouse. Means denoted by the same letter did not differ significantly according to Tukey's test ($P < 0.05$).

heterodimer comprised of LCB1 and LCB2 subunits in *Arabidopsis*, mutations in either subunit may affect its enzymatic activity, thus relieving SAMT-induced PCD. Both *fbr11-1* (a weak mutant allele in *AtLCB1*) and *Atlcb2a-1* (a T-DNA insertion mutant) failed to induce PCD when challenged by FB1 (Saucedo-Garcia *et al*., 2011; Shi *et al*., 2007). In addition, a smaller subunit of SPT termed ssSPT, which interacts with LCB1/LCB2 subunits, has been demonstrated to strongly influence the activity of SPT, and the sensitivity to FB1 was increased by *ssSPT* overexpression and reduced by *ssSPT*-RNA interference in *Arabidopsis* (Kimberlin *et al*., 2013).

The involvement of free sphingoid bases, the downstream products of SPT, in FB1-induced PCD has been widely reported, and the diminished SPT activity led to attenuated accumulation of these molecules (Saucedo-Garcia *et al*., 2011; Shi *et al*., 2007). Among the free sphingoid bases species, the most representative ones are sphinganine and phytosphingosine, which showed gradual and significant increase starting at early time of FB1 exposure (Saucedo-Garcia *et al*., 2011; Shi *et al*., 2007). In the case of *fbr11-1* and *Atlcb2a-1*, although the absence of AtLCB1 or AtLCB2a subunit did not affect the basal levels of free sphingoid bases, it resulted in less increase in free sphingoid bases upon FB1 treatment than the WT (Saucedo-Garcia *et al*., 2011; Shi *et al*., 2007). In present study, we found that *FBR41* had a mutation in *AtLCB2b* encoding an essential subunit of SPT. Similar to *fbr11-1* and *Atlcb2a-1*, *fbr41* produced lower levels of sphinganine and phytosphingosine after FB1 treatment compared with the WT (Figure 3b). One possibility is that SPT activity is reduced due to the loss of function in AtLCB2b. However, this

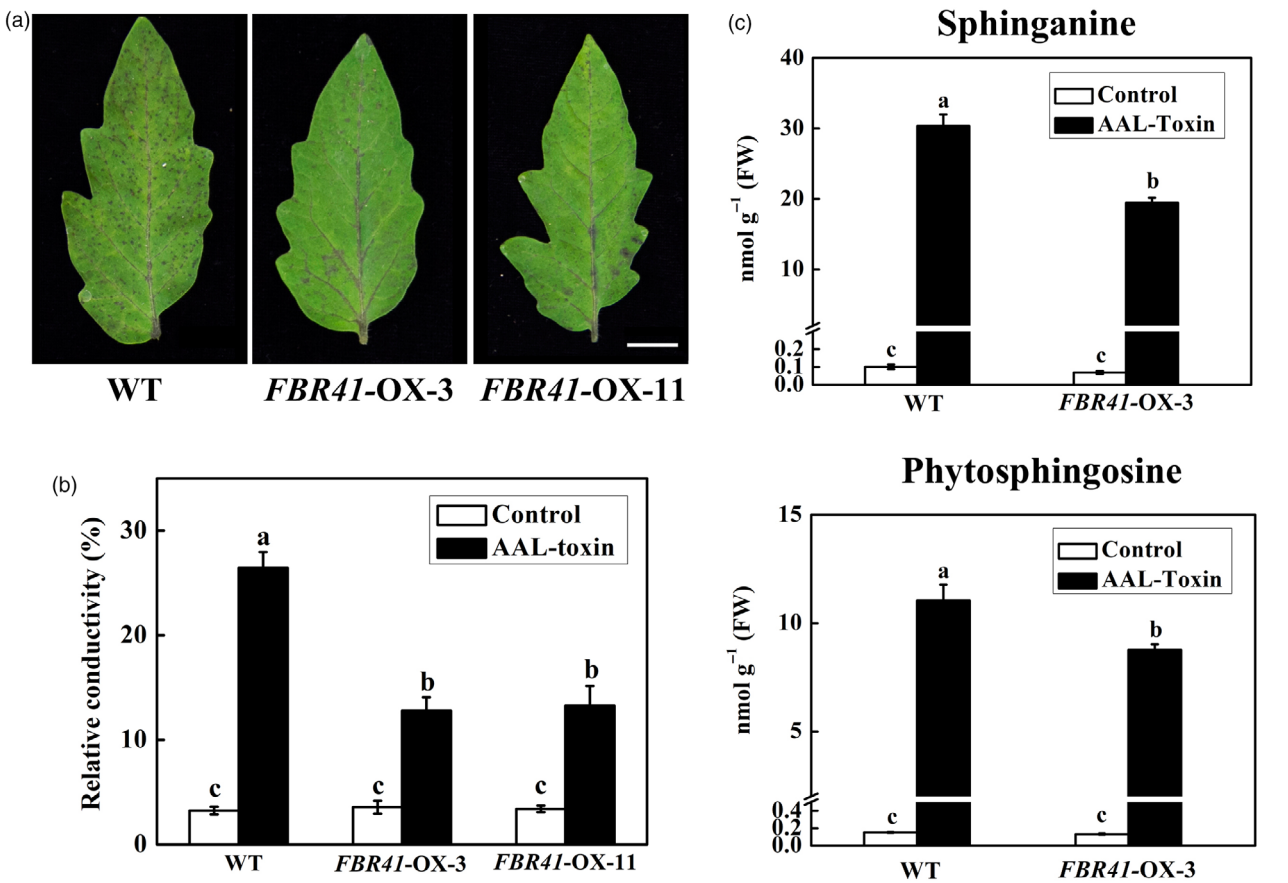

Figure 6 Effect of *FBR41* overexpression on resistance to AAL-toxin and free sphingoid bases contents in tomato leaflets. (a) Symptom of detached leaflets of wild-type (WT) and transgenic plants after AAL-toxin treatment. Detached leaflets of 5-week-old plants were incubated with 0.2 μM AAL-toxin under continuous light at 25 °C for 48 h and photographed. Scale bar = 1 cm. (b,c) Relative conductivity (b) and free sphingoid bases content (c) in leaflets of WT and transgenic plants after 48 h of AAL-toxin or control treatment. Data shown are means ± SD of three biological replicates. Different letters denote a statistically significant difference among treatments (one-way ANOVA, $P < 0.05$, Tukey's test). FW, fresh weight.

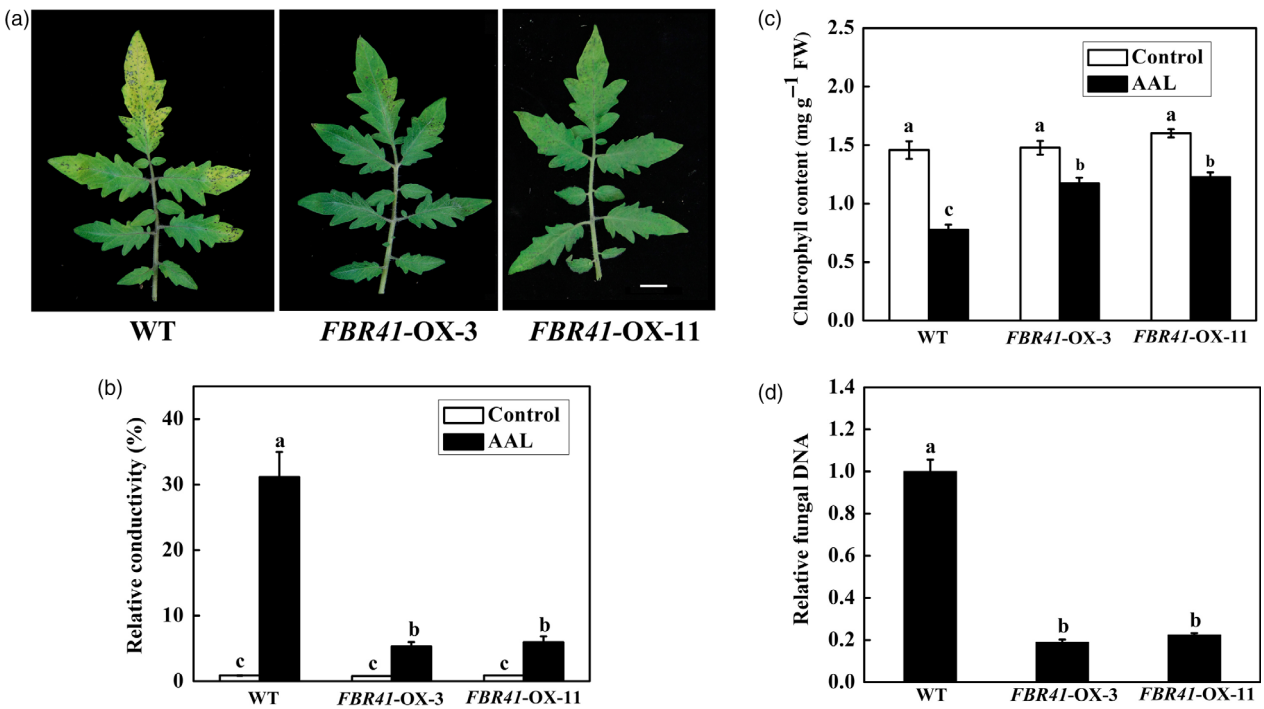

Figure 7 *FBR41*-overexpressing tomato plants show resistance to *Alternaria* stem canker. (a) The symptom of wild-type (WT) and *FBR41*-overexpressing tomato plants after AAL inoculation. Five-week-old plants were inoculated with AAL, and representative 4th leaves were photographed at 3 days postinoculation (DPI). Scale bar = 1 cm. (b–d) Relative conductivity (b), total chlorophyll content (c) and relative fungal DNA amount (d) in leaves of WT and transgenic plants at 3 DPI. In (d), the amount of fungal DNA was quantified by quantitative RT-PCR using *ALT1*-specific primers. Data shown are means ± SD of three biological replicates. Different letters denote a statistically significant difference among treatment (one-way ANOVA, $P < 0.05$, Tukey's test). FW, fresh weight.

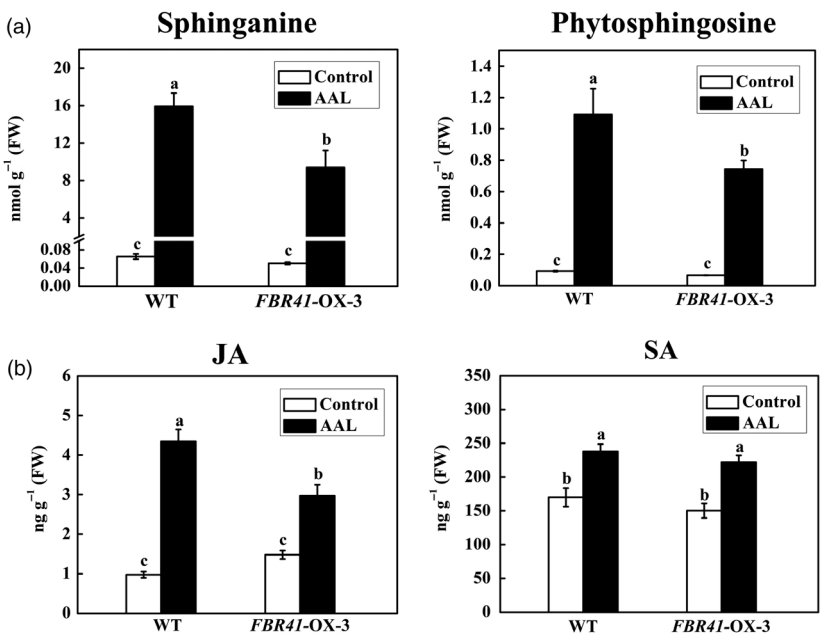

Figure 8 Contents of free sphingoid bases and phytohormones in wild-type (WT) and *FBR41*-overexpressing tomato plants under *Alternaria alternata* f. sp. *lycopersici* (AAL) infection. (a,b) The contents of free sphingoid bases (a) and jasmonate (JA) and salicylic acid (SA) (b) in WT and *FBR41*-overexpressing tomato plants with AAL treatment or control (0.1% Tween 20) at 3 days postinoculation (DPI). Data shown are means ± SD of three biological replicates. Different letters denote a statistically significant difference among treatments (one-way ANOVA, $P < 0.05$, Tukey's test).

possibility could be ruled out because *Arabidopsis* has two functionally redundant genes (*AtLCB2a* and *AtLCB2b*) that encode functional isoforms of LCB2 subunits, the expression level of *AtLCB2a* is higher than *AtLCB2b* (Dietrich *et al*., 2008; Saucedo-Garcia *et al*., 2011), suggesting that AtLCB2a plays a dominant role in maintaining SPT activity. Moreover, the null mutant of *AtLCB2b-1* did not display resistance to FB1 (Figure S1). Another possibility might be that FBR41 affects the combination of functional subunits, possibly through competing with functional AtLCB2 subunit for binding AtLCB1, yielding a dysfunctional AtLCB1/FBR41 heterodimer. The following clues are in support of this assumption. Firstly, *FBR41* is a dominant mutant

allele as the F_1 progeny from *fbr41* and WT was resistant to FB1 (Figure 1e). Additionally, the conserved pyridoxal phosphate-binding motif and lys residue in AtLCB2, which are essential for SPT function, are absent in FBR41 (Figure S2). Furthermore, luciferase complementation assays show that FBR41 interacts with AtLCB1 *in vivo* (Figure 4a–c), and FBR41 competes with AtLCB2a for binding to AtLCB1 (Figure 4d–f). Finally, we measured the SPT activity of microsomes prepared from leaves of WT and *fbr41* mutant. The data showed that *in planta* SPT activity in *fbr41* was approximately 70% of that in WT, either in untreated (Figure S3a) or in FB1-treated (Figure S3b) condition. Based on above evidence, it is concluded that FBR41 might produce a dysfunctional SPT by competing with functional AtLCB2a subunit in AtLCB1 binding, thus attenuating the accumulation of free sphingoid bases and enhancing the resistance to FB1 (Figure S4).

In addition to regulation of SAMT-induced PCD, SPT is also involved in plant growth and development (Chen *et al*., 2006; Dietrich *et al*., 2008; Teng *et al*., 2008). Suppression of *AtLCB1* and silencing of *AtLCB2b* in an *Atlcb2a* mutant background resulted in growth retardation, suggesting the crucial role of SPT in plant vegetative growth (Chen *et al*., 2006; Dietrich *et al*., 2008). In current survey, reduced plant size was observed in *fbr41* and *FBR41*-overexpressing *Arabidopsis* compared to WT (Figures 1d and 2d). Such findings are explicable, because SPT is suppressed in *fbr41* (Figure S3a), theoretically accompanied by decreased level of free sphingoid bases. To maintain the free sphingoid base pool, plants may restrict their growth. This possibility is supported by the fact that basal levels of free sphingoid bases in *fbr41* or *FBR41*-overexpressing *Arabidopsis* plants were similar to that in WT (Figure 3b). However, no obvious growth retardation was observed in *FBR41*-overexpressing tomato plants (Figure 5c), demonstrating a divergent effect of *FBR41* on plant vegetative growth in different species. It is probable that plant growth is marginally altered in *FBR41*-overexpressing tomato plants, which is difficult to distinguish from the WT plants. Also, we cannot rule out the possibility that *FBR41*-overexpressing tomato plants might adopt other strategy, instead of restricting vegetative growth, to replenish the reduced availability of free sphingoid bases.

The potential application of *FBR41* in crop improvement for enhanced resistance to SAMT-induced cell death was verified by ectopic overexpression of *FBR41* in phylogenetically distant tomato plants. *FBR41* positively regulates the resistance to AAL-toxin in tomato (Figure 6a) without pleiotropic effects on tomato growth and development (Table 1; Figure 5c–e). AAL-toxin-induced PCD is associated with the accumulation of free sphingoid bases, and prevention of this process can efficiently alleviate cell death. Chemical treatment with myriocin inhibited the activity of SPT, partially relieving the elevation of free sphingoid bases, therefore enhancing the resistance of tomato to AAL-toxin (Spassieva *et al*., 2002). The *Asc-1* partially restored the block on sphingolipid synthesis, thereby preventing the AAL-toxin-induced cell death (Brandwagt *et al*., 2000, 2002; Spassieva *et al*., 2002). In *FBR41*-overexpressing tomato plants, we also observed a suppressed elevation in free sphingoid bases upon AAL-toxin treatment, which might partially account for enhanced resistance to AAL-toxin-induced PCD (Figure 6b).

Tomato stem canker is a devastating disease worldwide and causes severe economic losses for tomato producers. The necrotrophic pathogen AAL is the causal agent of the disease (Grogan *et al*.,1975; Kohmoto *et al*., 1982; Malathrakis, 1983). In AAL-tomato interaction systems, AAL has evolved some pathogenic strategies to plunder the host. Previous reports have revealed the participation of JA signalling pathway in susceptibility of tomato to AAL (Egusa *et al*., 2009; Jia *et al*., 2013). In present study, *FBR41*-overexpressing tomato plants exhibited reduced accumulation of JA in response to AAL (Figure 8b), which might prevent the invasion of AAL into the host, thus leading to less fungal biomass and reduced disease symptom (Figure 7a–c). After successful invasion, AAL secretes a host-specific pathogenicity factor AAL-toxin, which causes marked accumulation of free sphingoid bases and induces cell death of the host (Abbas *et al*., 1994; Wang *et al*., 1996; Zhang *et al*., 2011). However, elevation of free sphingoid bases in *FBR41*-overexpressing tomato plants after AAL infection was attenuated compared to that in WT plants (Figure 8a). This might explain the less extent of cell death in *FBR41*-overexpressing plants. Taken together, *FBR41* might play a double role in improvement of tomato for enhanced resistance to *Alternaria* stem canker: inhibition of JA biosynthesis to prevent pathogen invasion and attenuation of free sphingoid base accumulation to suppress cell death.

During the whole lifespan, plants are exposed to broad range of pathogens, including necrotrophic and biotrophic pathogens according to their lifestyles. *Pseudomonas syringae* pv. tomato DC3000 (*Pst* DC3000) is a common type of (hemi) biotrophic pathogen, which causes bacterial speck disease in tomato. Interestingly, *FBR41*-overexpressing tomato plants displayed increased susceptibility to *Pst* DC3000 (Figure S6), indicating that *FBR41* functions differently in resistance against necrotrophic and biotrophic pathogens, but the underlying mechanism remains to be addressed in further studies.

SAMT contamination in certain agricultural commodities has been a growing concern for animal and human health, and SAMT-producing pathogens are a serious threat to crop production (Wang *et al*., 2006). As a dominant gene, *FBR41* is easier to be manipulated to inhibit pathogen invasion and reduce SAMT-induced cell death, therefore specifically reducing mycotoxin contamination in agricultural products and controlling the diseases caused by SAMT-producing pathogens.

Experimental procedures

Plant materials and growth conditions

Arabidopsis thaliana plants in Columbia (Col-0) ecotype were used in this study. *fbr41* was identified from an EMS-generated mutant population; the details were described in Methods S1. Previously characterized T-DNA insertional mutants *Atlcb2a-1* (SALK_061472) and *Atlcb2b-1* (SALK_110242) (Dietrich *et al*., 2008; Teng *et al*., 2008) were kindly provided by Dr Jianru Zuo (Chinese Academy of Sciences, Beijing, China).

AAL-sensitive tomato (*Solanum lycopersicum*) cultivar was obtained from Tomato Genetics Resource Center (University of California, Davis, CA), which was used for *FBR41* transformation.

Arabidopsis seeds were surface sterilized and imbibed in water at 4 °C for 3 days, then sown on half-strength MS medium containing 1% (w/v) sucrose and 0.7% (w/v) agar and cultivated at 22 °C under a 10-h light/14-h dark photoperiod. After 2 weeks, seedlings were transferred to pots containing a mixture of peat: vermiculite: perlite (6:3:1, v/v/v) and maintained in the same condition for 4 weeks.

Tomato seeds were germinated on wet filter paper and transferred to the aperture disc filled with a mixture of peat: vermiculite (2:1, v/v). The seedlings were grown under a 16-h

light/8-h dark photoperiod with the temperature of 26 °C in phytotron. After 3 weeks, seedlings were transplanted into plastic pot filled with the same substrate formula, which were watered every two days and fertilized at regular intervals. The plants were allowed to grow either in phytotron for characterization of plant height, morphology and leaf size and resistance to AAL-toxin and AAL or in the glasshouse for evaluation of flowering time, fruit development and yield.

Nicotiana benthamiana were grown in the same conditions as tomato seedlings, and plants at 5–6 leaf stages were used for transient transformation.

Mapping and cloning of *FBR41*

SSLP markers evenly distributed on chromosomes were selected to determine the approximate location of the mutation. For fine mapping, a total of 2500 FB1-resistant individuals from F_2 generations of a cross between *fbr41* and *Landsberg erecta* were used for PCR-based mapping with CAPS markers. The candidate gene within mapping interval was amplified using genomic DNA of *fbr41* and WT as template and sequenced. Primers used in this study were listed in Tables S2–S4.

Plasmid construction and plant transformation

To generate the *35S::FBR41-myc* construct, the coding sequence (CDS) of *FBR41* was amplified from *fbr41* cDNA (Primers listed in Table S4) and cloned into pQBV3 entry vector and combined with Gateway binary vector pGWB17 (35S promotor, c-4myc) (Nakagawa *et al.*, 2007). The resulting vectors were transformed into *Agrobacterium tumefaciens* strain GV3101 and LBA4404 for *Arabidopsis* and tomato transformation, respectively.

Arabidopsis transformation was performed by a floral dip procedure (Clough and Bent, 1998). Transformants were selected on half-strength MS agar medium containing Kanamycin. Homozygous T_3 transgenic lines were used for phenotype characterization.

The details of *Agrobacterium*-mediated tomato transformation were described in Methods S2. To identify positive T_0 transgenic plants, PCR analysis was performed using genomic DNA as template and gene-specific forward primer *FBR41*-F and vector-specific reverse primer *MYC*-R (Table S4). The number of T-DNA inserts was assumed by the separation rate at about 3:1 in T_1 generation on selective medium (half-strength MS agar medium containing 50 mg/L kanamycin). Five independent transgenic lines with single copy were selected, and their seeds (T_2 generation) were sown on selective medium to identify homozygous lines.

RNA isolation and gene expression analysis

Total RNA was extracted from plant leaves using TRIzol reagent (Invitrogen, Carlsbad, CA) according to the manufacturer's protocols. Genomic DNA was removed with RNA-free DNase I (Takara Bio, Otsu, Shiga, Japan). RNA (1 μg) was reverse-transcribed into cDNA with PrimeScript™ RT Reagent Kit (Takara) following the manufacturer's instructions. Quantitative RT-PCR was performed as previously described (Miao *et al.*, 2013). Semi-quantitative RT-PCR was performed using *FBR41*-specific primers and *SlACTIN7* as an internal control. PCR condition was 94 °C for 2 min followed by 30 cycles of 98 °C for 10 s, 50 °C for 30 s and 68 °C for 20 s. PCR fragments were analysed on 1.5% agarose gel and visualized with a UV transilluminator. The primers used for gene expression analysis are listed in Table S4.

Extraction and quantification of free sphingoid bases, JA and SA

Measurement of free sphingoid bases was performed as previously described (Bielawski *et al.*, 2009) with minor modifications. Briefly, approximately 500 mg of rosette leaves from 6-week-old plants was homogenized and fortified with the internal standards (C17 base D-erythro-sphingosine, Avanti Polar Lipids, Alabaster, AL), which was extracted with ethyl acetate/isopropanol/H_2O (6:3:1, v/v/v) solvent. After evaporation, the samples were dissolved in 0.5 mL methanol and analysed by Agilent 6460 Triple Quadrupole LC/MS/MS system (Agilent, Palo Alto, CA) using an Agilent ZORBAX SB-C18 (150 × 2.1 mm, 3.5 μM particle size column, with 2 mM ammonium acetate containing 0.1% formic acid/methanol mobile phase system). Peaks for target analytes and internal standards were collected and processed with the Agilent Masshunter Quantitative Analysis software. Quantitative analyses of free sphingoid bases were based on the analyte specific calibration curves, generated by plotting the analyte/internal standard peak area ratio against analyte concentrations. SPT is a key enzyme of biosynthetic pathway of free sphingoid bases, and measurement of its activity was described in Methods S4.

Extraction and quantification of JA and SA was performed as previously reported (Pan *et al.*, 2008) with minor modifications. In brief, approximately 0.3 g leaves were ground into powder in liquid nitrogen, and 1.5 mL of isopropanol/H_2O/concentrated HCL (2:1:0.005, v/v/v) solvent with 10 ng internal standard (D5-JA, C/D/N Isotopes, Pointe-Claire, PQ, Canada; D4-SA, Toronto Research Chemicals, Toronto, ON, Canada) was added, followed by agitation for 30 min at 4 °C. 1.5 mL of CH_2Cl_2 was added, followed by agitation for 30 min at room temperature and then centrifugation at 12 000 ***g*** for 5 min. After centrifugation, the supernviaould-like liquid was collected, evaporated and dissolved in 200 μL of methanol/H_2O (3:2, v/v) solvent. The samples were analysed by Agilent 6460 Triple Quadrupole LC/MS/MS system. Peaks for JA/SA molecule and internal standard were collected and processed with Agilent Masshunter Quantitative Analysis software. The amount of JA and SA was determined by comparison of response to the corresponding internal standard.

Luciferase complementation imaging (LCI) assays

The LCI assay was performed as previously described (Chen *et al.*, 2008) with minor modifications. To assay the interaction between FBR41 and AtLCB1, *FBR41* CDS and *AtLCB1* CDS were amplified by PCR with primers containing appropriate restriction site and inserted into pCAMBIA-nLUC (35S promotor, c-Nluc) and pCAMBIA-cLUC (35S promotor, n-Cluc), respectively. To assay the impact of FBR41 on the interaction of AtLCB1 and AtLCB2a, *AtLCB1* CDS and *AtLCB2a* CDS were amplified by PCR and cloned into pCAMBIA-cLUC and pCAMBIA-nLUC, respectively. Meanwhile, the *35S::FBR41-myc* construct was used for transient transformation and its corresponding empty vector was used as control. The primers used for vector construction were listed in Table S4. *Agrobacterium* strain GV3101 harbouring the indicated constructs were grown in Luria–Bertani (LB) medium at 28 °C overnight and then transferred to new LB medium supplemented with 10 mM MES (pH 5.6) and 40 μM acetosyringone (1:100, v/v) for 16 h. After centrifugation, the cell pellets were resuspended with agroinfiltration buffer (10 mM $MgCl_2$, 0.2 mM acetosyringone) to an OD_{600} of 1.5. Equal volumes of *Agrobacterium* suspension were mixed and infiltrated into *N. benthamiana* leaves. After infiltration, plants

were incubated at 26 °C for 72 h with 16-h light/8-h dark before the luciferase activity measurement. Low-light cooled CCD imaging apparatus NightOWL II LB983 (Belthold, Bad Wildbad, Germany) with Indigo software was used to capture the luciferase image. The leaves were sprayed with 0.5 mM D-luciferin (Promega, Madison, WI) and placed in darkness for 5 min before luminescence detection. Relative luminescence was used for the comparison of luciferase activity.

Western blot

Protein extraction was carried out as previously described (An *et al*., 2017). The agroinfiltrated parts of *N. benthamiana* leaves were harvested, and the leaf tissue was ground in liquid nitrogen resuspended in protein extraction buffer containing 50 mM Tris–HCl (pH 7.5), 150 mM NaCl, 0.1% Triton X-100, 0.2% Nonidet P-40, 0.6 mM PMSF, 20 mM MG132, 5 μM DTT and protease inhibitor mixture (Roche, Rotkreuz, Switzerland), and placed on ice for 30 min. After centrifuge (4 °C, 12 000 ***g***, 20 min), the supernatants were collected and total protein concentration was quantified using Bradford method (Beyotime, Haimen, China) following the manufacturer's protocols.

For Western blot analysis, samples were denatured using SDS loading buffer, separated by 10% SDS-PAGE and then transferred onto a polyvinylidene fluoride membrane (Millipore, Billenca, MA). For detection of nLUC- or cLUC-fusion protein, the membrane was incubated with the rabbit anti-firefly luciferase antibody (Abcam, Cambridge, UK), which reacts with both N-terminal fragment and C-terminal fragment of LUC, followed by a horseradish peroxidase (HRP)-conjugated goat anti-rabbit IgG secondary antibody (Abmart, Arlington, MA). For detection of FBR41-myc protein, a mouse anti-c-MYC antibody (Abmart) was used as a primary antibody and a HRP-conjugated goat anti-mouse IG was used as the secondary antibody. After antibody incubation, the membrane was visualized using an enhanced chemiluminescence (ELC) substrate kit (Fdbio science, Hangzhou, China) according to the manufacturer's instructions.

Abiotic and biotic stress treatment

For FB1 treatment, *Arabidopsis* seedlings were grown on half-strength MS medium containing 1.5 μL FB1 (Sigma-Aldrich, St. Louis, MO) or 0.15% methanol as control. *Arabidopsis* leaves were infiltrated with 10 μL FB1 solution as previously described (Zhao *et al*., 2015). AAL-toxin treatment of detached tomato leaflets was performed as previously described (Zhang *et al*., 2011). AAL toxin was a gift from Dr Liangcheng Du (Department of Chemistry, University of Nebraska, Lincoln, NE, USA).

AAL infection was performed according to Jia *et al*. (2013) with minor modifications. In brief, leaves of 5-week-old tomato plants were sprayed with AAL spore suspensions containing approximately 1.0×10^6 spores/mL or 0.1% (v/v) Tween 20 as control, then maintained at high humidity at 26 °C and a 16-h light/8-h dark photoperiod. Disease symptoms emerged about 3–4 days after infection. *Pseudomonas syringae* pv tomato DC3000 infection assays were described in Methods S3.

Measurement of cell death, fungal biomass and chlorophyll content

Cell death was measured with an electrolyte leakage assay according to Gechev *et al*. (2004). Measurement of fungal biomass was performed as previously described (Jia *et al*., 2013). The primer pairs DeH-F and E8T7 (Table S4) designed for the amplification of AAL-toxin biosynthesis gene (*ALT1*) were used for detecting AAL. Estimation of chlorophylls was carried out according to the procedure of Arnon (1949).

Statistical analysis

Statistical analysis was performed using the SPSS package program version 19.0.0 (SPSS Inc., Chicago, IL). Data were analysed by one-way ANOVA followed by Turkey's test at a 95% confidence level ($P < 0.05$) or Student's *t*-test at 99.9% confidence level ($P < 0.001$). The values were reported as means with standard deviation (SD) for all the results.

Acknowledgements

We are grateful to Tomato Genetics Resource Center (University of California, Davis, CA, USA) for providing AAL-sensitive tomato cultivar, Dr Jianru Zuo (Chinese Academy of Sciences, Beijing, China) for providing T-DNA insertional mutants *Atlcb2a-1* (SALK_061472) and *Atlcb2b-1* (SALK_110242), Dr Liangcheng Du (University of Nebraska, Lincoln, NE, USA) for providing AAL-toxin, and Dr Steffen Abel (Leibniz-Institute of Plant Biochemistry, Halle, Germany) for critical reading. This work was supported by the Ministry of Agriculture of China (2016ZX08009003-001), National Natural Science Foundation of China (31200230, 31601746) and Zhejiang Provincial Natural Science Foundation of China (LZ15C150001).

Conflict of interest

The authors declare that they have no conflict of interests.

Author contributions

QW, JW, YZ and ZS planned and designed the research. ZS, YZ, SC, FM, HL and SH performed the experiments and analysed data. CL provided EMS-generated mutants and guided map-based cloning. ZS, QW, LL, YZ and JW wrote the manuscript. ZS and YZ contributed equally.

References

Abbas, H.K., Tanaka, T., Duke, S.O., Porter, J.K., Wray, E.M., Hodges, L., Sessions, A.E. *et al*. (1994) Fumonisin- and AAL-Toxin-induced disruption of sphingolipid metabolism with accumulation of free sphingoid bases. *Plant Physiol.* **106**, 1085–1093.

Akamatsu, H., Itoh, Y., Kodama, M., Otani, H. and Kohmoto, K. (1997) AAL-Toxin-deficient mutants of *Alternaria alternata* tomato pathotype by restriction enzyme-mediated integration. *Phytopathology*, **87**, 967–972.

An, C., Li, L., Zhai, Q., You, Y., Deng, L., Wu, F., Chen, R. *et al*. (2017) Mediator subunit MED25 links the jasmonate receptor to transcriptionally active chromatin. *Proc. Natl Acad. Sci. USA*, **114**, E8930–E8939.

Arnon, D.I. (1949) Copper enzymes in isolated chloroplasts. Polyphenoloxidase in beta vulgaris. *Plant Physiol.* **24**, 1–15.

Bielawski, J., Pierce, J.S., Snider, J., Rembiesa, B., Szulc, Z.M. and Bielawska, A. (2009) Comprehensive quantitative analysis of bioactive sphingolipids by high-performance liquid chromatography-tandem mass spectrometry. *Methods Mol. Biol.* **579**, 443–467.

Brandwagt, B.F., Mesbah, L.A., Takken, F.L., Laurent, P.L., Kneppers, T.J., Hille, J. and Nijkamp, H.J. (2000) A longevity assurance gene homolog of tomato mediates resistance to *Alternaria alternata* f. sp. *lycopersici* toxins and fumonisin B1. *Proc. Natl Acad. Sci. USA*, **97**, 4961–4966.

Brandwagt, B.F., Kneppers, T.J., Nijkamp, H.J. and Hille, J. (2002) Overexpression of the tomato *Asc-1* gene mediates high insensitivity to AAL toxins and fumonisin B1 in tomato hairy roots and confers resistance to

Alternaria alternata f. sp. *lycopersici* in *Nicotiana umbratica* plants. *Mol. Plant Microbe Interact.* **15**, 35–42.

Chen, M., Han, G., Dietrich, C.R., Dunn, T.M. and Cahoon, E.B. (2006) The essential nature of sphingolipids in plants as revealed by the functional identification and characterization of the *Arabidopsis* LCB1 subunit of serine palmitoyltransferase. *Plant Cell*, **18**, 3576–3593.

Chen, H., Zou, Y., Shang, Y., Lin, H., Wang, Y., Cai, R., Tang, X. *et al*. (2008) Firefly luciferase complementation imaging assay for protein-protein interactions in plants. *Plant Physiol.* **146**, 368–376.

Chen, M., Cahoon, E.B., Saucedo-García, M., Plasencia, J. and Gavilanes-Ruíz, M. (2010) Plant sphingolipids: structure, synthesis and function. In *Lipids in Photosynthesis: Essential and Regulatory Functions* (Wada, H. and Murata, N., eds), pp. 77–115. Dordrecht: Springer Netherlands.

Clough, S.J. and Bent, A.F. (1998) Floral dip: a simplified method for Agrobacterium-mediated transformation of *Arabidopsis thaliana*. *Plant J.* **16**, 735–743.

Das, A., Kawai-Yamada, M. and Uchimiya, H. (2010) Programmed cell death in plants. In *Abiotic Stress Adaptation in Plants: Physiological, Molecular and Genomic Foundation* (Pareek, A., Sopory, S.K. and Bohnert, H.J., eds), pp. 371–383. Dordrecht: Springer Netherlands.

Dietrich, C.R., Han, G., Chen, M., Berg, R.H., Dunn, T.M. and Cahoon, E.B. (2008) Loss-of-function mutations and inducible RNAi suppression of *Arabidopsis LCB2* genes reveal the critical role of sphingolipids in gametophytic and sporophytic cell viability. *Plant J.* **54**, 284–298.

Egusa, M., Ozawa, R., Takabayashi, J., Otani, H. and Kodama, M. (2009) The jasmonate signaling pathway in tomato regulates susceptibility to a toxin-dependent necrotrophic pathogen. *Planta*, **229**, 965–976.

Gechev, T.S., Gadjev, I.Z. and Hille, J. (2004) An extensive microarray analysis of AAL-toxin-induced cell death in *Arabidopsis thaliana* brings new insights into the complexity of programmed cell death in plants. *Cell. Mol. Life Sci.* **61**, 1185–1197.

Glazebrook, J. (2005) Contrasting mechanisms of defense against biotrophic and necrotrophic pathogens. *Annu. Rev. Phytopathol.* **43**, 205–227.

Grogan, R.G., Kimble, K.A. and Misaghi, I. (1975) A stem canker disease of tomato caused by *Alternaria alternata* f. sp. *lycopersici*. *Phytopathology*, **65**, 880–886.

Hanada, K. (2003) Serine palmitoyltransferase, a key enzyme of sphingolipid metabolism. *Biochim. Biophys. Acta*, **1632**, 16–30.

Ikushiro, H., Hayashi, H. and Kagamiyama, H. (2001) A water-soluble homodimeric serine palmitoyltransferase from *Sphingomonas paucimobilis* EY2395^{T} strain. Purification, characterization, cloning, and overproduction. *J. Biol. Chem.* **276**, 18249–18256.

Jia, C., Zhang, L., Liu, L., Wang, J., Li, C. and Wang, Q. (2013) Multiple phytohormone signalling pathways modulate susceptibility of tomato plants to *Alternaria alternata* f. sp. *lycopersici*. *J. Exp. Bot.* **64**, 637–650.

Kimberlin, A.N., Majumder, S., Han, G., Chen, M., Cahoon, R.E., Stone, J.M., Dunn, T.M. *et al*. (2013) *Arabidopsis* 56-amino acid serine palmitoyltransferase-interacting proteins stimulate sphingolipid synthesis, are essential, and affect mycotoxin sensitivity. *Plant Cell*, **25**, 4627–4639.

Kohmoto, K., Verma, V.S., Nishimura, S., Tagami, M. and Scheffer, R.P. (1982) New outbreak of *Alternaria* stem canker of tomato in Japan and production of host-selective toxins by the causal fungus. *Anim. Behav.* **72**, 1405–1416.

Lachaud, C., Prigent, E., Thuleau, P., Grat, S., Da Silva, D., Briere, C., Mazars, C. *et al*. (2013) 14-3-3-regulated Ca$^{(2+)}$-dependent protein kinase CPK3 is required for sphingolipid-induced cell death in *Arabidopsis*. *Cell Death Differ.* **20**, 209–217.

Lynch, D.V. and Dunn, T.M. (2004) An introduction to plant sphingolipids and a review of recent advances in understanding their metabolism and function. *New Phytol.* **161**, 677–702.

Malathrakis, N.E. (1983) *Alternaria* stem canker of tomato in Greece. *Phytopathol. Mediterr.* **22**, 33–38.

Meena, M., Zehra, A., Dubey, M.K., Aamir, M., Gupta, V.K. and Upadhyay, R.S. (2016) Comparative evaluation of biochemical changes in tomato (*Lycopersicon esculentum* Mill.) infected by *Alternaria alternata* and its toxic metabolites (tea, AOH, and AME). *Front. Plant Sci.* **7**, 1408.

Mesbah, L.A., Kneppers, T.J., Takken, F.L., Laurent, P., Hille, J. and Nijkamp, H.J. (1999) Genetic and physical analysis of a YAC contig spanning the fungal disease resistance locus *Asc* of tomato (*Lycopersicon esculentum*). *Mol. Gen. Genet.* **261**, 50–57.

Mesbah, L.A., van der Weerden, G.M., Nijkamp, H.J.J. and Hille, J. (2000) Sensitivity among species of *Solanaceae* to AAL toxins produced by *Alternaria alternata* f.sp *lycopersici*. *Plant. Pathol.* **49**, 734–741.

Miao, H., Wei, J., Zhao, Y., Yan, H., Sun, B., Huang, J. and Wang, Q. (2013) Glucose signalling positively regulates aliphatic glucosinolate biosynthesis. *J. Exp. Bot.* **64**, 1097–1109.

Nakagawa, T., Kurose, T., Hino, T., Tanaka, K., Kawamukai, M., Niwa, Y., Toyooka, K. *et al*. (2007) Development of series of gateway binary vectors, pGWBs, for realizing efficient construction of fusion genes for plant transformation. *J. Biosci. Bioeng.* **104**, 34–41.

Pan, X., Welti, R. and Wang, X. (2008) Simultaneous quantification of major phytohormones and related compounds in crude plant extracts by liquid chromatography-electrospray tandem mass spectrometry. *Phytochemistry*, **69**, 1773–1781.

Saucedo-Garcia, M., Guevara-Garcia, A., Gonzalez-Solis, A., Cruz-Garcia, F., Vazquez-Santana, S., Markham, J.E., Lozano-Rosas, M.G. *et al*. (2011) MPK6, sphinganine and the *LCB2a* gene from serine palmitoyltransferase are required in the signaling pathway that mediates cell death induced by long chain bases in *Arabidopsis*. *New Phytol.* **191**, 943–957.

Shi, L., Bielawski, J., Mu, J., Dong, H., Teng, C., Zhang, J., Yang, X. *et al*. (2007) Involvement of sphingoid bases in mediating reactive oxygen intermediate production and programmed cell death in *Arabidopsis*. *Cell Res.* **17**, 1030–1040.

Spassieva, S.D., Markham, J.E. and Hille, J. (2002) The plant disease resistance gene *Asc-1* prevents disruption of sphingolipid metabolism during AAL-toxin-induced programmed cell death. *Plant J.* **32**, 561–572.

Tamura, K., Mitsuhashi, N., Hara-Nishimura, I. and Imai, H. (2001) Characterization of an *Arabidopsis* cDNA encoding a subunit of serine palmitoyltransferase, the initial enzyme in sphingolipid biosynthesis. *Plant Cell Physiol.* **42**, 1274–1281.

Teng, C., Dong, H., Shi, L., Deng, Y., Mu, J., Zhang, J., Yang, X. *et al*. (2008) Serine palmitoyltransferase, a key enzyme for *de novo* synthesis of sphingolipids, is essential for male gametophyte development in *Arabidopsis*. *Plant Physiol.* **146**, 1322–1332.

Walton, J.D. (1996) Host-selective toxins: agents of compatibility. *Plant Cell*, **8**, 1723–1733.

Wang, H., Li, J., Bostock, R.M. and Gilchrist, D.G. (1996) Apoptosis: a functional paradigm for programmed plant cell death induced by a host-selective phytotoxin and invoked during development. *Plant Cell*, **8**, 375–391.

Wang, Q., Wang, J., Yu, F., Zhu, X., Kathia, Z.R. and Du, L. (2006) Mycotoxin fumonisins: health impacts and biosynthetic mechanism. *Prog. Nat. Sci.* **16**, 7–15.

Zhang, L., Jia, C., Liu, L., Zhang, Z., Li, C. and Wang, Q. (2011) The involvement of jasmonates and ethylene in *Alternaria alternata* f. sp. *lycopersici* toxin-induced tomato cell death. *J. Exp. Bot.* **62**, 5405–5418.

Zhao, Y., Wang, J., Liu, Y., Miao, H., Cai, C., Shao, Z., Guo, R. *et al*. (2015) Classic myrosinase-dependent degradation of indole glucosinolate attenuates fumonisin B1-induced programmed cell death in *Arabidopsis*. *Plant J.* **81**, 920–933.

Supporting information

Additional supporting information may be found online in the Supporting Information section at the end of the article.

Figure S1 Lesion formation upon fumonisin B1 (FB1) injection in *fbr41* and null mutants for *AtLCB2a* and *AtLCB2b*.

Figure S2 Comparison of amino acid sequences of FBR41, AtLCB2b and AtLCB2a.

Figure S3 *In planta* SPT activity in wild-type (WT) and *fbr41* mutant.

Figure S4 Proposed model considering the role of FBR41 in the resistance to sphinganine analog mycotoxin (SAMT)-induced cell death.

Figure S5 The disease symptoms of wild-type (WT) and *FBR41*-overexpressing transgenic plants after AAL inoculation.
Figure S6 *FBR41*-overexpressing tomato exhibited decreased resistance against *Pseudomonas syringae* pv. tomato DC 3000 (*Pst* DC3000).
Table S1 Fumonisin B1-resistant mutants identified by forward genetic screening in *Arabidopsis*.
Table S2 List of SSLP markers used for first-pass mapping.
Table S3 List of CAPS markers used for fine mapping.
Table S4 Primers used in this study.
Methods S1 Screening of the fumonisin B1-resistant mutant.
Methods S2 Tomato transformation.
Methods S3 *Pseudomonas syringae* pv tomato DC3000 infection assays.
Methods S4 Microsome preparation and SPT assay.

